JMEPEG (2010) 19:1220–1224
DOI: 10.1007/s11665-010-9600-x

1059-9495/$19.00

Kinetics of Nanoscale Cerium Dioxide Prepared by Pechini Process

Teng Zhang, Dian Tang, Yanqun Shao, and Zhenping Yu

(Submitted July 29, 2008)

The crystallization kinetics of nanoscale cerium dioxide particles prepared by Pechini method was investigated by various non-isothermal methods using differential scanning calorimetry. The activation energies for the crystallization calculated from modified Kissinger and Ozawa equations are 19.7 and 22.4 kJ/mol, respectively, which are much lower than that of solid-state reaction. The Avrami exponent calculated from Ozawa equation is about 1.5, indicating that the nucleation process is controlled by long-range diffusion in the early stage, and the small nuclei grow into various shapes. The nucleation rate decreases as the reaction proceeds. In addition, the kinetics of crystal growth was also studied.

Keywords advanced characterization, electron microscopy, heat treating

1. Introduction

Nanocrystalline cerium dioxide (CeO_2) has numerous applications in photo catalysts, oxygen sensors, solid electrolytes in solid oxide fuel cell, and ultraviolet absorbers (Ref 1-3). Most of these applications depend on the morphologies of the nanocrystallines, which make the morphology-controllable synthesis necessary for tapping in full potential of CeO_2.

Many methods have been developed for the fabrication of nanocrystalline cerium compounds such as sol-gel process, hydrothermal process, chemical vapor deposition, and electrodeposition methods (Ref 4-8). Particularly, sol-gel method including Pechini method attracts the greatest attention due to its simplicity and precise control at the atomic/molecular level of materials.

However, few studies have been carried out on the crystallization kinetics of nanoscale CeO_2, which is critical for the particle size of CeO_2 and hence its performance. Recently, the doping of CoO was found to decrease the activation energy and Avrami factor of CeO_2 prepared by solid-state reaction process (Ref 9).

In this article, attention has been focused on the kinetics of the crystallization process as well as the crystal growth of nanoscale CeO_2 prepared by Pechini process.

2. Experimental Procedure

Chemical reagents including Cerium (III) nitrate ($Ce(NO_3)_3 \cdot 6H_2O$), citric acid, and ethylene glycol were mixed at a certain ratio. The mixed precursor was stirred for 12 h to obtain the homogeneous sol. After drying at 100 °C in air for several days, the transparent sol changed into yellowish brown powders. The powders were then heat treated at 300, 450, 600, and 750 °C for 1 h. The powders were finally crushed and sieved to 90-106 μm.

Differential scanning calorimetry (DSC; Model DT-40, Shimadzu, Japan) was conducted at the heating rates of 10, 20, 30, and 40 °C/min. The crystallized samples were characterized using by x-ray diffraction (XRD; XD-5A diffractometer, Shimadzu, Japan), with Cu-K_α source (λ = 1.5406 Å). The averaged size of crystalline was calculated by Scherrer equation, $D = k\lambda/(\beta\cos\theta)$, where k is taken as 0.9 for cubic structure, λ is the wavelength of x-ray irritation, β is the peak width at half-maximum height, and θ is the diffraction angel of the (111) peak of CeO_2. A small amount of CeO_2 was suspended in ethanol solution, and then spread on the carbon-coated copper grids for transmission electron microscopy analysis (TEM; model JEOL-2000EX, Japan).

3. Theoretical Analysis

3.1 Crystallization Kinetics

Non-isothermal methods are often favored for the kinetics study because of their operational simplicity and convenience, compared with isothermal models, in addition to being less time consuming. However, the validity of the non-isothermal approaches, i.e., Kissinger plot or Ozawa equation was challenged by many researchers who argued that the crystallization process should be described by nucleation and crystal growth process, in stead of the *n*th-order reaction. In addition, they also mentioned that those equations derived from JMA equation are not suitable for non-isothermal process since the JMA equation describes the isothermal condition. A modified form of the Kissinger model, introduced by Matusita and Sakka (Ref 10, 11), distinguished crystallization processes that occur on a fixed number of nuclei from those where nucleation and crystal growth occur simultaneously. In addition, the role of crystallization mechanism was taken into

Teng Zhang, Dian Tang, and **Yanqun Shao**, Institute for Materials Research, Fuzhou University, Fuzhou, Fujian 350002, China; and **Zhenping Yu**, Fujian Center for Analysis and Testing, Fuzhou, Fujian 350003, China. Contact e-mails: tzmq3@mst.edu and tangdian@fzu.edu.cn.

account in this approach to get the meaningful kinetic information.

Based on the nucleation and crystallization process, the following equation was obtained:

$$\ln[-\ln(1-x)] = -n\ln\beta - 1.052\left(\frac{mE}{RT}\right) + C, \quad \text{(Eq 1)}$$

where x is the crystallization fraction at a given temperature, β is the heating rate in DSC, E is the activation energy for crystallization, C is the constant, m and n are numerical factors that depend on the crystallization mechanism, and T is the temperature at which crystallization fraction (x) is measured for all the curves. The values of m and n are equal for the special case in which the surface crystallization is predominant.

In order to get the value of n, the above equation can be written in the following form, which is well known as Ozawa equation (Ref 12):

$$\left.\frac{d\{\ln[-\ln(1-x)]\}}{d\ln\beta}\right|_T = -n. \quad \text{(Eq 2)}$$

Equation 1 could also be written in another form to obtain the activation energy as follows:

$$\ln\beta = -1.052\left(\frac{mE}{nRT}\right) - \left\{\frac{\ln[-\ln(1-x)]}{n}\right\} + C. \quad \text{(Eq 3)}$$

In addition, T can be replaced by T_p because the volume fraction of crystallization at the peak temperature (T_p) is independent of the heating rate. Thus, the plot of ln β versus $1/T_p$ yields the modified Ozawa plot.

Solving Eq 3 for the $d\,(dx/dt)/dt = 0$, the following equation is obtained:

$$\ln\frac{T_p^2}{\beta^n} = -1.052\left(\frac{mE}{RT_p}\right) + C. \quad \text{(Eq 4)}$$

Thus, the plot of $\ln(T_p^2/\beta^n)$ versus $1/T_p$ yields the modified Kissinger plot.

3.2 Kinetics of Crystal Growth

According to the theory of phase transformation, the rate of crystal growth can be described as follows (Ref 13):

$$\mu = C[\exp(-Q/KT)][1-\exp(-\Delta Fv/KT)], \quad \text{(Eq 5)}$$

where μ is the rate of crystal growth, C is the constant, ΔFv is the molar free energy for crystallization, Q is the activation energy for crystal growth, and K is the molar gas constant.

For amorphous solids, it is known that $\Delta Fv \gg KT$. Then Eq 5 can be simplified into

$$\mu = C[\exp(-Q/KT)]. \quad \text{(Eq 6)}$$

On the other hand, if the crystal growth is assumed to take place at a constant rate,

$$d = \mu t \quad \text{(Eq 7)}$$

then the particle size of crystals (d) at a given time can be obtained as follows:

$$\ln d = -Q/KT + a, \quad \text{(Eq 8)}$$

where a is a constant.

4. Results and Discussion

The DSC curve of CeO_2 as synthesized at the heating rate of 40 °C/min is shown in Fig. 1. An exothermal peak occurs at 95 °C, which corresponds to the decomposition of organic and desorption of water. Another exothermal peak at 270 °C is caused by the crystallization of CeO_2. The peak temperatures of the crystallization for CeO_2 are 238, 250, and 258 °C at the heating rate of 10, 20, and 30 °C/min, respectively.

The XRD patterns for those CeO_2 powders heat treated at 300, 450, and 600 °C for 1 h are shown in Fig. 2. The diffraction peaks, occurring at $2\theta = 28.5°$, 47.4°, 56.3°, and 69.5°, correspond to the crystal planes of CeO_2, namely (111), (220), (311), and (301), respectively. Most of the diffraction peaks of CeO_2 appear in the sample heat treated at 300 °C, indicating that the crystallization almost completes after holding at 300 °C for 1 h. Some other peaks, in the XRD patterns, might be caused by the contaminations during the heat treated process or the crushing process. In addition, the

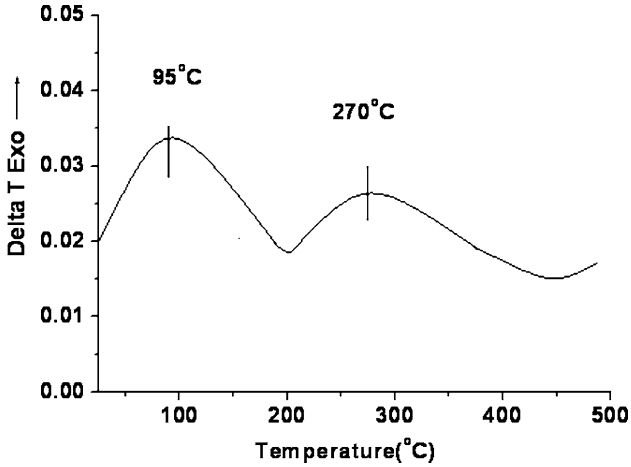

Fig. 1 DSC curve of CeO_2 as synthesized at the heating rate of 40 °C/min

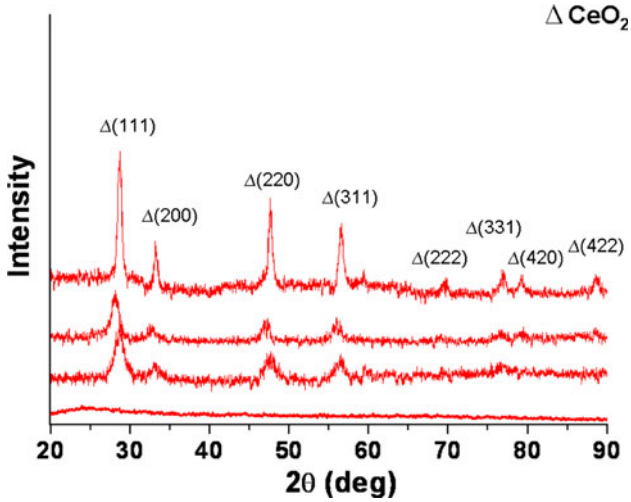

Fig. 2 X-ray diffraction patterns at (a) as synthesized, (b) 300 °C, (c) 450 °C, and (d) 600 °C for 1 h

diffraction peaks of CeO_2 powders become sharper after the heat treatment at higher temperatures, indicating that the particle size of CeO_2 crystalline increases with increasing temperature. The calculated size of crystalline is 6 nm, for the heat-treated sample at 300 °C for 1 h, based on the Scherrer equation. Similarly, the calculated size of crystalline is 11 and 45 nm, for the heat-treated samples at 450 and 700 °C for 1 h, respectively.

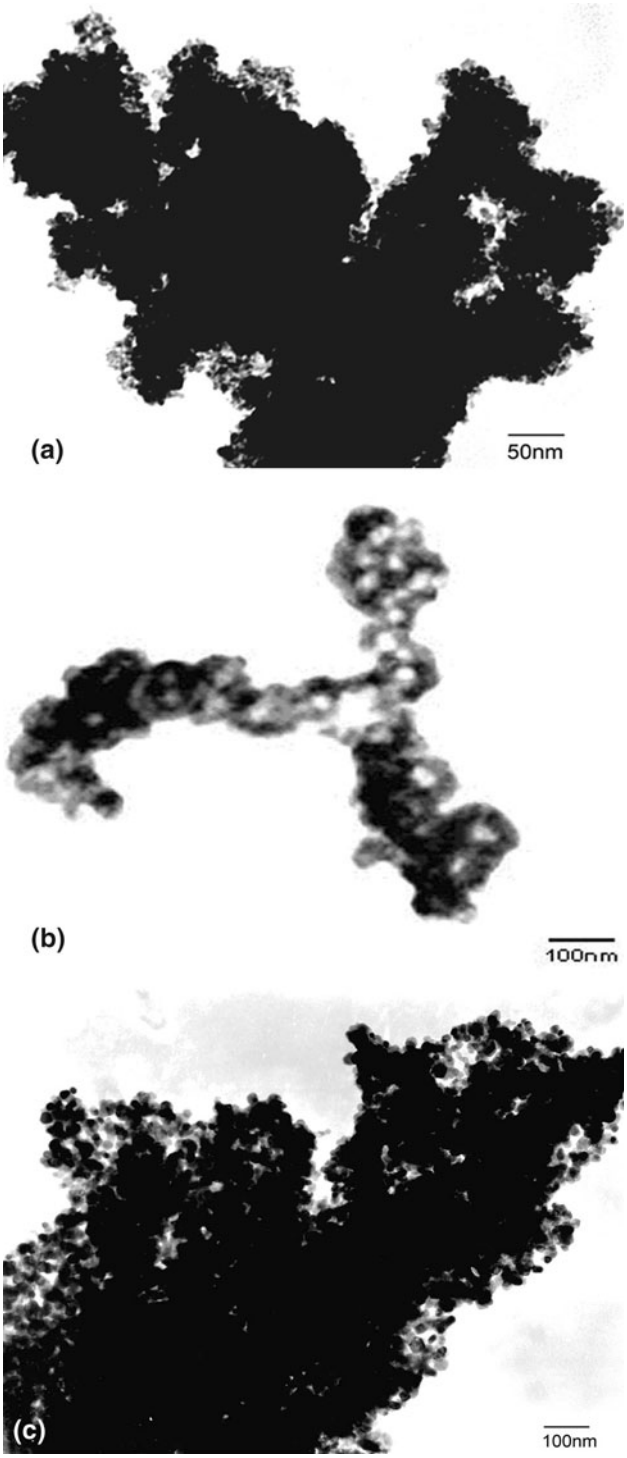

Fig. 3 TEM patterns of CeO_2 heat treated at (a) 450 °C, (b) 600 °C, and (c) 750 °C for 1 h

The TEM patterns for the samples heat treated at 450, 600, and 750 °C for 1 h are shown in Fig. 3. The morphology of samples changes from dendrite to "τ" and to plate, with increasing temperature. The measured particle size of samples is ~10 and ~50 nm at 450 and 750 °C, respectively, in spite of the agglomeration of fine particles. This result is in consistent with that of Fig. 2 using Scherrer equation.

The exponent n was calculated from the results of DSC using Eq 2 (T = 250 °C in this study). There are two reasons for choosing 250 °C as the target temperature. First of all, the crystalline already forms at 250 °C based on the result of Fig. 2. In addition, the small particle size can be obtained with the heat treatment at low temperature, which is beneficial for the electro-catalyst application (Ref 14). Figure 4 shows the plot of $\ln[-\ln(1-x)]$ versus $\ln\ \beta$. The peak areas of crystallization in each DSC curve were measured using the planimeter. Then, the value of fraction crystallized, x, at various heating rates was calculated from the ratio of the partial area to total area under the crystallization peak. The slope of this plot is 1.5. According to the literature (Ref 13), n = 1.5 indicates the surface nucleation. The nucleation process is controlled by long-range diffusion in the early stage, and the small nuclei grow into different shapes. The nucleation rate decreases as the reaction proceeds. This result is consistent with the different morphologies as shown in Fig. 3. In addition, this mechanism (n = 1.5) is different from the mechanism observed in solid-state reaction (n = 3) (Ref 9), which corresponds to the bulk nucleation, and the nucleation rate decreases to zero after initial nucleation.

The activation energy associated with the crystallization of CeO_2 can be calculated using Eq 3. Figure 5 shows the plot $\ln\beta$ versus $1/T_p$. The value of $1.052(mE/nR)$ is obtained from the slope. The activation energy calculated from modified Ozawa equation is 22.4 kJ/mol, since $m = n$ (surface nucleation predominates) in this case.

Similarly, the plot of $\ln(T_p^2/\beta_n)$ versus $1/T_p$ gives a straight line shown in Fig. 6. The slope is $1.052(mE/R)$ based on Eq 4. From Fig. 6, the activation energy is 19.7 kJ/mol, since m = 1.5 ($m = n$ when surface nucleation predominates).

Therefore, the activation energy of crystallization for the CeO_2 prepared by Pechini process is much lower than that prepared by solid-state reaction, namely, 697 kJ/mol (Ref 9). The low activation energy for the crystallization of CeO_2 in this

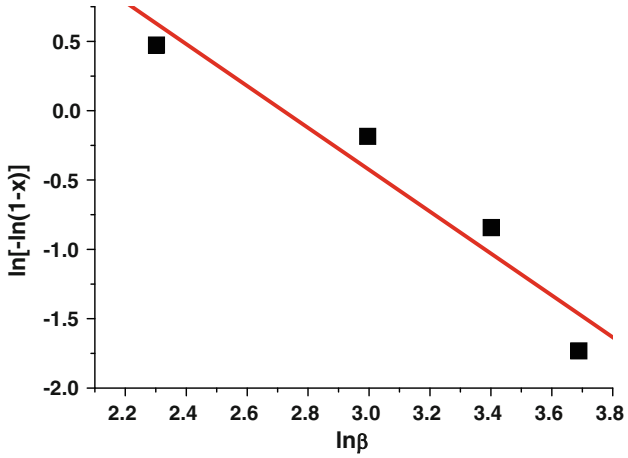

Fig. 4 Ozawa plot to determine the n at 250 °C

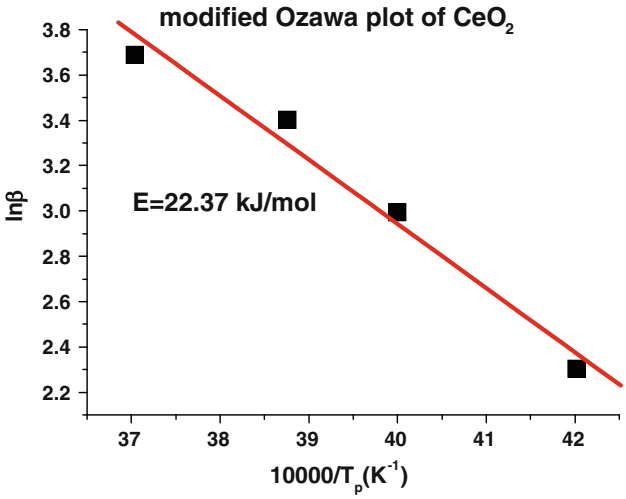

Fig. 5 Plot of ln β vs. $1/T_p$ (modified Ozawa plot)

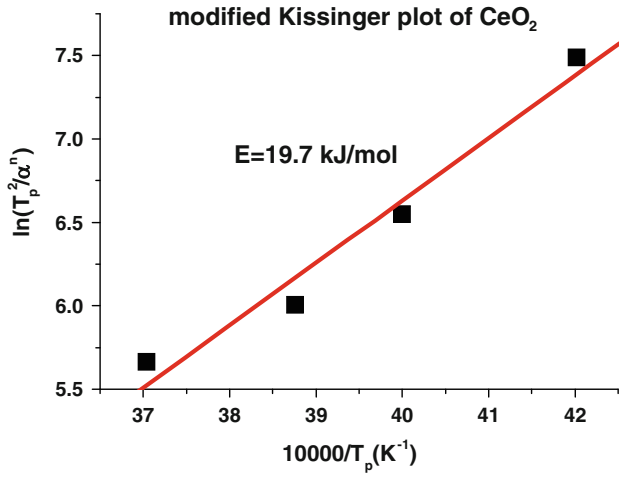

Fig. 6 Ln(T_p^2/β_n) vs. $1/T_p$ (modified Kissinger plot)

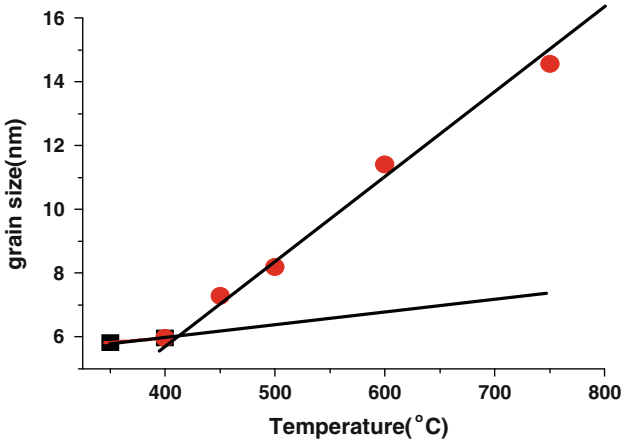

Fig. 7 Calculated size of CeO_2 crystalline vs. temperature

study can be related to the high surface energy of nanoscale particles made by Pechini process. In addition, the diffusion in the sol is much faster than that in solid-state reaction, which might also contribute to the low activation energy of crystallization in Pechini process. The small activation energy for crystallization again confirms that nanocrystalline of CeO_2 can be formed at 250 °C by Pechini approach.

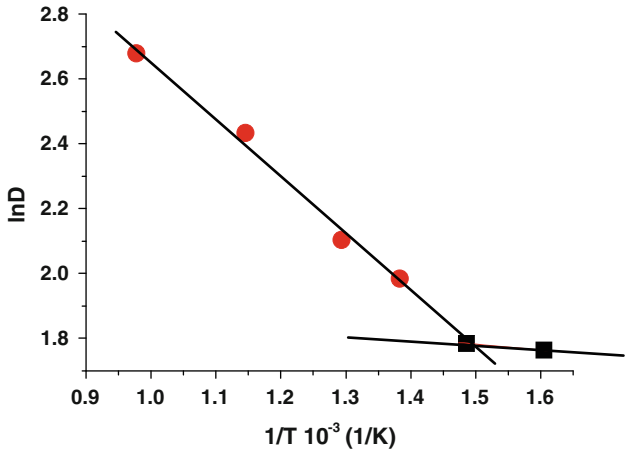

Fig. 8 Ln D vs. $1/T$

Figure 7 shows the calculated size of CeO_2 crystalline heat treated at 300, 350, 400, 450, 500, 600, and 750 °C for 1 h, using the Scherrer equation. Clearly, there are two steps below and above 400 °C in the plot, indicating that two processes occur in different temperature ranges.

The plot of ln D versus $1/T$ using Eq 8 is shown in Fig. 8. The activation energies of crystal growth below and above 400 °C are 1.5 and 14.8 kJ/mol, respectively. This change in growth rate may be caused by the changes of material properties such as status and structures as the temperature increases (Ref 13).

5. Conclusions

The crystallization of nanoscale CeO_2 in Pechini system was studied using modified non-isothermal methods. The Avrami exponent is 1.5, indicating that the surface nucleation is predominant. The activation energies for crystallization, calculated from the modified Kissinger and Ozawa equations, are 19.7 and 22.4 kJ/mol, respectively, which are much lower than that of solid-state reaction. The activation energies of crystal growth below and above 400 °C are 1.5 and 14.8 kJ/mol, respectively.

Acknowledgment

This study was financially supported by the Natural Science Foundation of China (No. 50472002).

References

1. M. Izaki, T. Saito, and M. Chigane, Low Temperature Deposition of Cerium Dioxide Film by Chemical Reaction, *J. Mater. Chem.*, 2001, **11**(8), p 1972–1978
2. T. Suzuki, I. Kosacki, and H.U. Anderson, Electrical Conductivity and Lattice Defects in Nanocrystalline Cerium Oxide Thin Films, *J. Am. Ceram. Soc.*, 2001, **84**(9), p 2007–2014

3. L. Madler, W.J. Stark, and S.E. Pratsinis, Flame-Made Ceria Nanoparticles, *J. Mater. Res.*, 2002, **17**(6), p 1356–1362
4. S. Chromik, M. Cannaerts, and S. Gazi, Influence of (1102) Sapphire Substrate on Structural Perfection of CeO_2 Thin Films, *Physica C*, 2002, **371**(4), p 301–308
5. M. Flytzani, Nanostructured Cerium Oxide "Ecocatalysts", *MRS Bull.*, 2001, **26**(11), p 885–889
6. X. Dong, Investigation on the Variation of Ce Valence State During the Formation of CeO_2 Nanometer Particles, *J. Chin. Ceram. Soc.*, 1997, **25**(3), p 323–327 (in Chinese)
7. X. Dong, J.H. Yan, and W. Yu, Preparation of Nanocrystalline CeO_2 by Hydrothermal Crystallization, *Rare Metal Mater. Eng.*, 2002, **31**(4), p 312–314 (in Chinese)
8. M.F. Luo, R. Lin, and M. Chen, Characterization and Preparation of Ce-Zr-O Solid Solution, *J. Chin. Rare Earth Soc.*, 2000, **18**(1), p 35–37 (in Chinese)
9. T. Zhang, P. Hing, and H. Huang, Sintering and Grain Growth of CoO-Doped CeO_2 Ceramics, *J. Eur. Ceram. Soc.*, 2002, **22**(1), p 27–34
10. K. Matusita and S. Sakka, Kinetic Study of Crystallization of Glass by Differential Thermal-Criterion on Application of Kissinger Plot, *J. Non-Cryst. Solids*, 1980, **38–39**(2), p 741–746
11. K. Matusita, T. Komatsu, and R. Yokota, Kinetics of Non-Isothermal Crystallization Process and Activation Energy for Crystal Growth in Amorphous Materials, *J. Mater. Sci.*, 1984, **19**(1), p 291–296
12. T. Ozawa, Kinetics of Non-Isothermal Crystallization, *Polymer*, 1971, **12**, p 150–158
13. E.D. Zanotto, The Applicability of the General Theory of Phase Transformations to Glass Crystallization, *Thermochim. Acta*, 1996, **280/281**, p 73–82
14. T. Zhang, D. Tang, Y. Shao, X. Ke, and S. You, Synthesis and Characterization of Nanoscale $Ce_{(x)}Ru_{(1-x)}O_2$ Coating with Electrochemical Activity, *J. Am. Ceram. Soc.*, 2007, **90**(3), p 989–992